

Supporting Information

Fluorinated PCPDTBT with Enhanced Open Circuit Voltage and Reduced Recombination for Highly Efficient Polymer Solar Cells

Steve Albrecht¹, Silvia Janietz², Wolfram Schindler³, Johannes Frisch⁴, Jona Kurpiers¹, Juliane Kniepert¹, Sahika Inal¹, Patrick Pingel¹, Konstantinos Fostiropoulos³, Norbert Koch⁴, and Dieter Neher^{1*}

¹ *Institut für Physik und Astronomie, Universität Potsdam, Karl-Liebknecht-Str. 24/25, 14476 Potsdam, Germany*

² *Fraunhofer Institut für Angewandte Polymerforschung, Geiselbergstr. 69, 14476 Potsdam, Germany*

³ *Helmholtz-Zentrum Berlin für Materialien und Energie GmbH, Hahn-Meitner-Platz 1, 14109 Berlin, Germany*

⁴ *Institut für Physik, Humboldt-Universität zu Berlin, Brook-Taylor-Str. 6, 12489 Berlin, Germany*

The supporting information contains the following data:

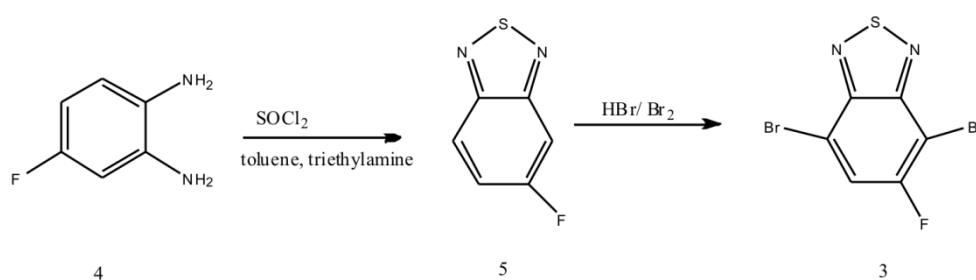
- materials and instrumentation for polymer synthesis
- details of the synthesis of the monomers and polymers
- Fig S1,S2: Molecular weight distribution of PCPDTBT and F-PCPDTBT
- Fig S3,S4: ¹H-NMR Spectra and TGA of F-PCPDTBT
- sample fabrication and testing
- Fig S5: Solution and thin film absorption spectra
- Fig S6: FET Output characteristics and SCLC measurements
- Fig S7: Histograms of the plasmon maps
- Fig S8: total-, pre- and collected charges for optimized blends measured at different delay times and pre-bias

* To whom correspondence should be addressed: neher@uni-potsdam.de

Materials and instrumentation for polymer synthesis and analysis

All reagents were purchased from Fluka or Aldrich Co. and used without further purification. All solvents are dried under standard conditions. Unless otherwise specified, $^1\text{H-NMR}$ spectra were recorded with a 500 MHz Varian INOVA 500 at 295 K in CDCl_3 as solvent. Elemental analysis was recorded with a EA 1110 CHNS-O from CE Instruments. Differential Scanning Calorimetry (DSC) was done on a Netzsch DSC 204 equipment under nitrogen with 10 mg polymer in 40 μl aluminum-pans using scan rates of 10 K/min. Microwave assisted polymerization was performed in a CEM discover LabMATETM microwave reactor. The molecular weight and polydispersity index (PDI) of the polymer were determined by high temperature gel permeation chromatography (GPC) using a Waters Alliance 2000 equipped with an RID detector (at Max Planck Institute of Polymer Research Mainz, Germany). Trichlorobenzene was used as eluent at 135°C and commercial polystyrenes were used as standards. Thermogravimetric analysis was performed with a Perkin Elmer Thermogravimetric Analyzer TGA 7.

Synthesis of 5-Fluoro-2,1,3-benzothiadiazol (5)



Scheme S1: Synthesis of 5-Fluoro-2,1,3-benzothiadiazol (5) and 4,7-dibromo-5-Fluoro-2,1,3-benzothiadiazole (3)

To a 250 ml round bottom flask containing 10.0 g (79.28 mmol) 4-fluoro-1,2-phenylenediamine, 100 ml toluene and 46.0 ml (327.6 mmol) triethylamine were added. This reaction mixture was cooled down with acetone/ N_2 . After that thionylchloride 12.0 ml (163.9 mmol) was slowly added. The reaction mixture was allowed to reflux for one hour. After cooling down to room temperature the mixture was given to ice water, diluted with toluene. The solid was filtered off and the filtrate was washed several times with water and dried with Mg SO_4 . After

filtration the toluene was evaporated and the remaining product was further purified by column chromatography on silicagel with hexane/ ethylacetate 10:1 as mobile phase. The yield was 43 %.

Elemental analysis: $C_6H_3N_2SF$ (154,17) Calcd. C: 46.74; H: 1.96; N: 18.18; S: 20.80; F: 12.32; Found: C 46.00; H: 1.85, N: 18.14; S: 20.84;

1H NMR (500 MHz, $CDCl_3$): δ ppm= 7.45 (dd, 1H); 7.60 (d, 1H); 8.00 (dd, 1H)

Synthesis of 4,7-Dibromo-5-Fluoro-2,1,3-benzothiadiazole (3)

5-Fluoro-2,1,3-benzothiadiazol 10.40 g (67.5 mmol) and 45.8 ml HBr were added in a 100 ml round bottom flask. After that bromine 11.1 ml was added dropwise. The reaction mixture was stirred for two days at 95°C and additionally two days at room temperature. The reaction mixture was put in water and the solid was filtered off, washed several times with water to be neutral and dried. The product was then recrystallized from methanol + 5% toluene. The yield was 33 %.

Elemental analysis: $C_6H_1Br_2N_2SF$ (311,96); Calcd. C:23.10; H: 0.32; N: 8.98; Br: 51.22 S: 10.28; F:6.09; Found C: 22.77; H: 0.31; N: 8.64; S: 10.61;

1H NMR (500 MHz, $CDCl_3$): δ ppm= 7.80 (d, 1H)

Synthesis of polymer PCPDTBT (P-H)

4,7-Dibromo-2,1,3-benzothiadiazole (2) 210.5 mg (0.7163 mol), 4,4-bis(2-ethylhexyl)-2,6-bis(trimethylstannyl)-4H-cyclopenta[2,1-b:3,4-benzo-thiadiazole] (1) 600mg (0.8238 mmol) and 4 ml of p-xylene containing $Pd(PPh)_3$ 20 mg (5mol% relative to Br) were charged in a microwave tube in the glove box and stirred for 30 min. After stirring the reagents for 30 min inside the glove box the tube was sealed and moved into the microwave reactor outside of the glove box. The following reaction conditions were then used: 120°C for 5min, 140°C for 5 min and 170°C for 40 min. The originated polymer solution was cooled down to about 60°C and precipitated into 300 ml methanol. The polymer was dissolved in $CHCl_3$ (200ml) and mixed with a solution of sodium diethyldithiocarbamate trihydrate (10g) in distilled water

(200ml). The mixture was strongly stirred at 80°C over night under nitrogen. The organic phase was separated and washed 3 times with water, dried over MgSO₄, filtrated and concentrated. The concentrated solution was again precipitated in CH₃OH. After drying the polymer was extracted with methanol (12h), hexan (6h), aceton (6h) and chloroform (6h) and precipitated again in methanol. The yield was 51%.

Poly[2,6-(4,4-bis(2-ethylhexyl)-4H-cyclopenta[2,1-b;3,4-b']dithiophene)-alt-4,7-(2,1,3-benzothiadiazole)] (**PCPDTBT = P-H**). $M_n = 10.9$ KDa, $M_w = 22.9$ KDa, PDI = 2.1.

¹H-NMR (500 MHz, 115°C, d₂-1,1,2,2-tetrachloroethane) : δ ppm = 8.4 – 7.0 (br m, 4H); 2.4 - 1.8 (br m, 4H); 1.6 - 0.4 (br m, 30H);

Elemental analysis: C₃₃H₄₄N₂S₃ (564.91) Calcd. C; 70.16; H; 7.85; N; 4.96; S; 17.03; Found: C; 69.31; H; 7.28; N; 4.86; S; 17.72

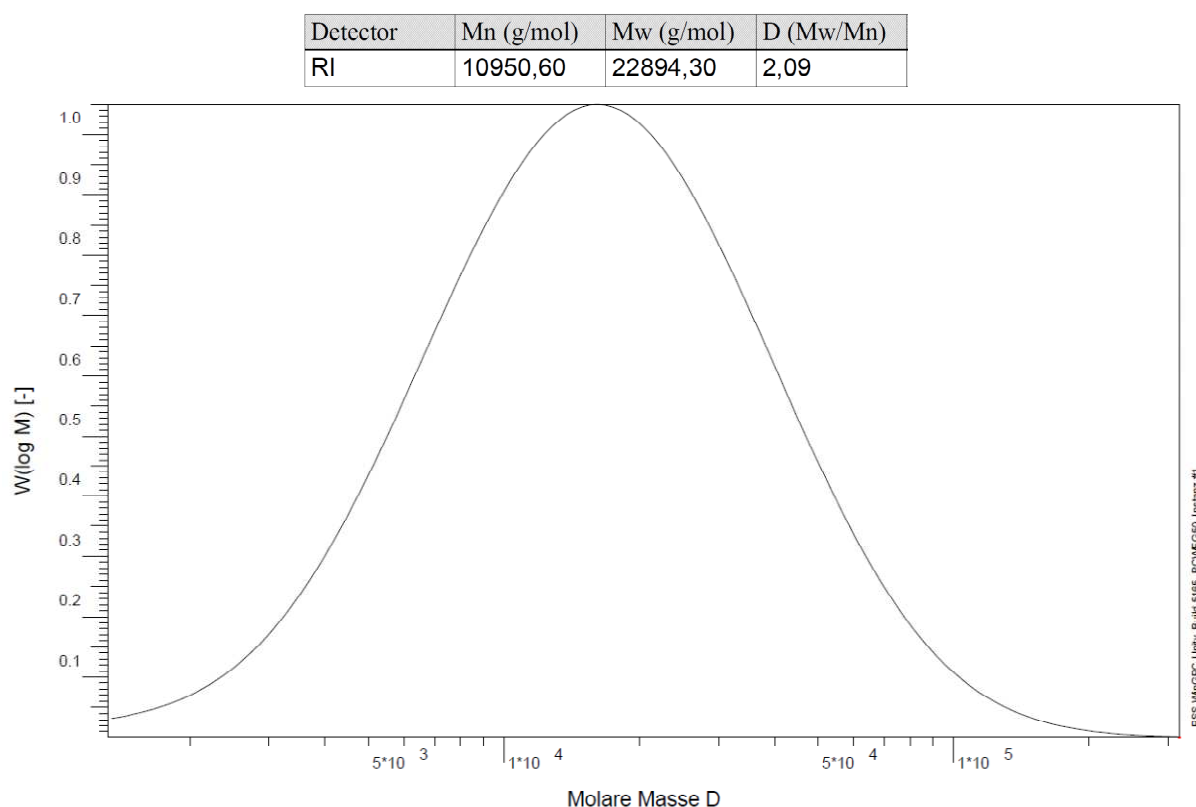


Fig. S1: Molecular weight distribution of PCPDTBT used in this work measured at 135°C in TCB against PS standards.

Synthesis of polymer F-PCPDTBT (P-F)

4,7-Dibromo-5-fluoro-2,1,3-benzothiadiazole (**3**) 363 mg (1.1640 mol), 4,4-bis(2-ethylhexyl)-2,6-bis(trimethylstannyl)-4H-cyclopenta[2,1-b:3,4-benzothiadiazole] (**1**) 975 mg (1.3387 mmol) and 6 ml of p-xylene containing Pd(PPh)₃₄ 32.5 mg (5 mol% relative to Br) were charged in an microwave tube in the glove box. The polymerization and purification were identical to the above described processes. The yield was 67%.

Poly[2,6-(4,4-bis(2-ethylhexyl)-4H-cyclopenta[2,1-b:3,4-benzothiadiazole)-alt-4,7-(5-F-2,1,3-benzothiadiazole)] (**F-PCPDTBT=P-F**). $M_n = 10.1$ KDa, $M_w = 21.5$ KDa, PDI = 2.13.

¹H-NMR (500 MHz, 115°C, d₂-1,1,2,2-tetrachloroethane) : δ ppm = 8.4 – 7.0 (br m, 3H); 2.4 – 1.8 (br m, 4H); 1.6 – 0.4 (br m, 30H)

Elemental analysis: C₃₃H₄₃FN₂S₃ (582.90) Calcd. C;68.00: H; 7.44: N; 4.81: S; 16.50: Found C;66.89: H; 6.87: N; 4.73: S; 17.12

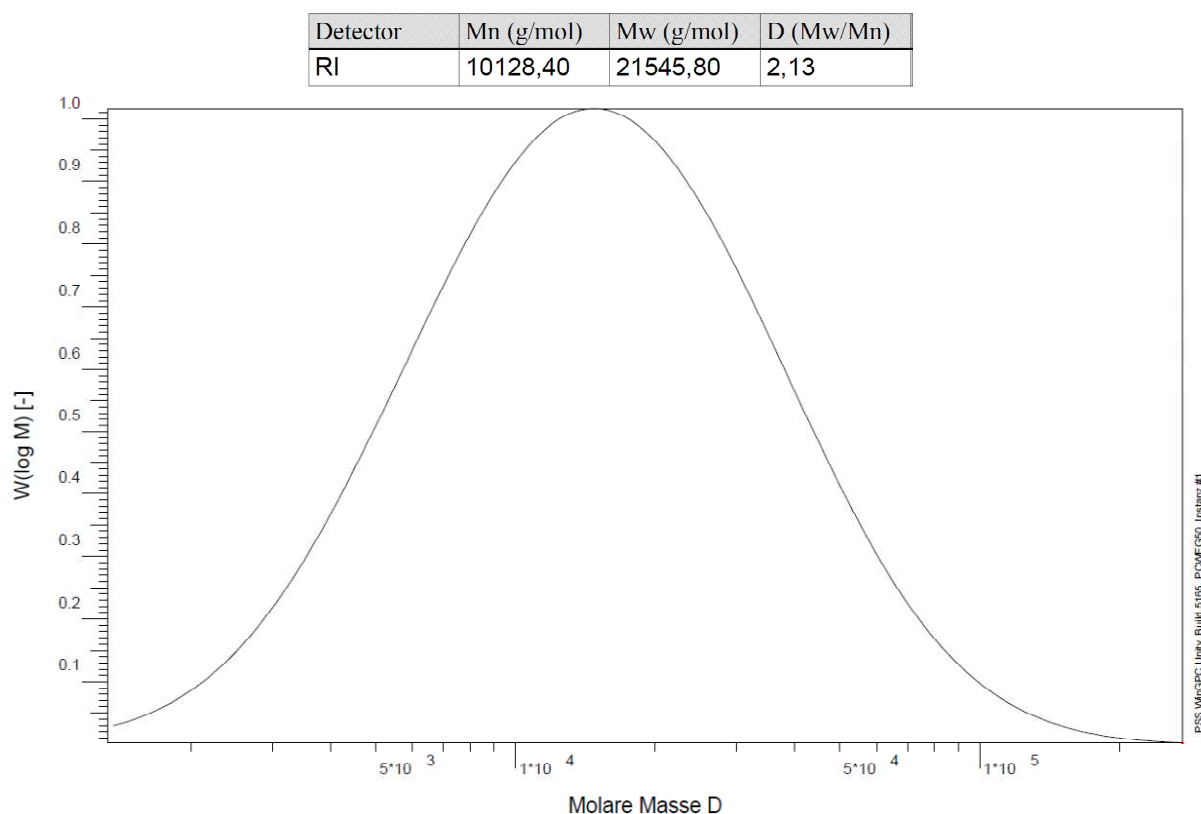


Fig. S2: Molecular weight distribution of F-PCPDTBT measured at 135°C in TCB against PS standards.

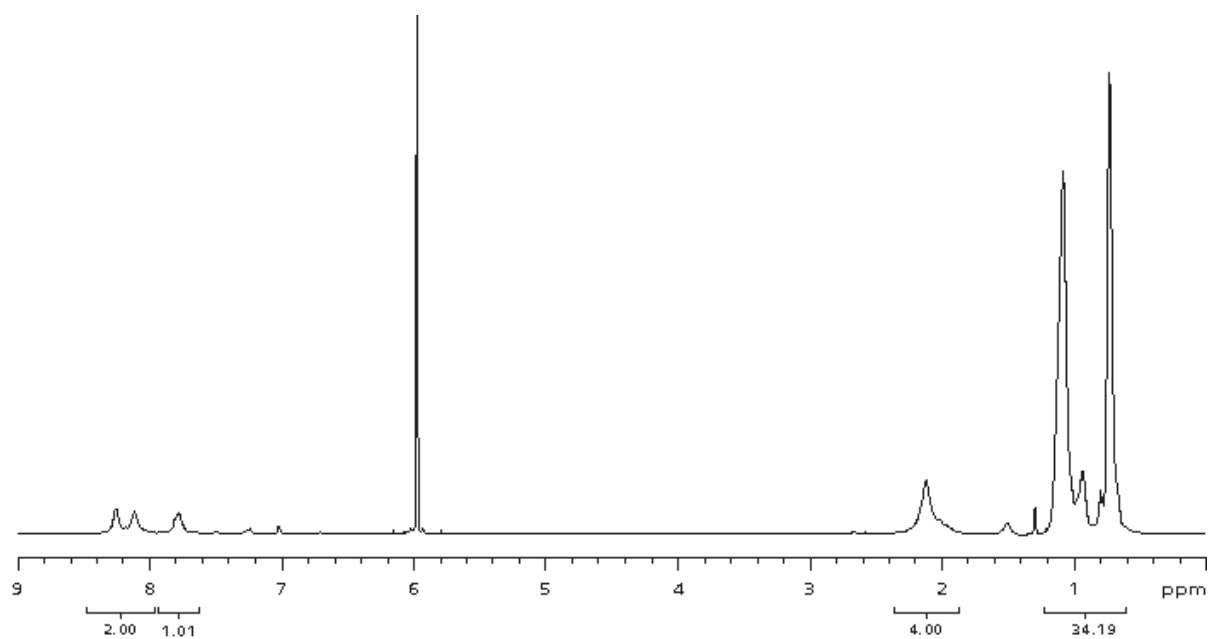


Fig. S3: ^1H -NMR spectra of F-PCPDTBT.

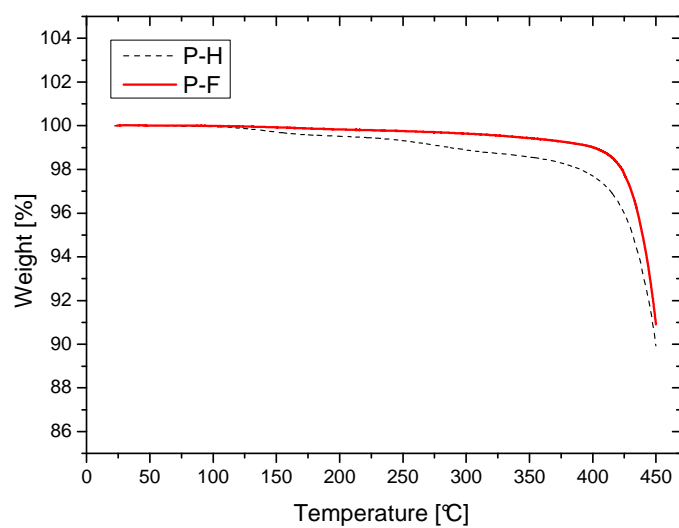


Fig. S4: Thermogravimetric analysis (TGA) of F-PCPDTBT (red) and PCPDTBT (black) used in this work.

Sample fabrication

Devices were fabricated on pre-structured ITO coated glass slides (Optrex) cleaned in acetone, detergent, DI-water, isopropanol and dried with a nitrogen gun. After that the ITO was plasma cleaned and subsequently a 40 nm layer of PEDOT (Clevios AI 4083) was spin cast on ITO. Annealing of the PEDOT:PSS was performed in a nitrogen filled glove-box at 180°C for 10 min. Unless otherwise mentioned, the active layer was spin cast from solutions containing 1 to 3 blend ratios (by weight) of P-H or P-F and PC₇₀BM (99%, Solenne). Chlorobenzene was used as the solvent processed with different amounts (0%; 1% or 3vol%) of diiodooctane (DIO). The total blend concentration was 36 mg/ml and spin coating was performed with 1400-1700 rpm for 40 sec to give active layer thicknesses between 90 and 100 nm. To complete the solar cell devices, 10 nm Ca and 100 nm Al were thermally evaporated with a base pressure below 10⁻⁶ mbar through shadow masks to define the active area to be 16 mm² for IPCE, 6.36 mm² for solar cell characteristics, and 1.1mm² for TDCF and Photo-CELIV. The small area for TDCF and photo-CELIV devices was used to realize a small RC-constant. Hole-only samples for SCLC measurements were prepared similar to solar cells but with MoO₃ (7 nm) and Ag (100 nm) electrodes with an active area of 4.91 mm². Bottom gate top-contact FETs were prepared on Si/SiO₂ wafer silanized using hexamethyldisilazane (HMDS) for 26 h at 60°C with a ca. 40 nm active layer thickness and MoO₃ (10 nm) and Ag (100 nm) interdigitated electrodes. Due to the high boiling point of DIO, all devices processed with DIO have been dried in vacuum at room-temperature for at least 5 h prior to evaporation, since residual DIO functions as a hole trap.¹ Samples for Photo-CELIV or TDCF have been encapsulated with two component epoxy resin and a glass lid prior to air exposure. For the UPS measurements, single polymer films and blends processed with 1 or 3vol% of DIO were prepared on ITO/PEDOT:PSS identical to the solar cell samples but with smaller thicknesses of 10-20 nm. For EFTEM 50-70 nm thick blend films on

ITO/PEDOT:PSS were used. These films were then floated off in de-ionized water and picked up with the TEM-grid.

Absorption Spectroscopy

All absorption measurements were performed on a Varian Cary 5000 UV-VIS-NIR absorption spectrometer using a double beam transmission mode. In this mode one beam contains the sample and the other a reference sample to subtract the background absorption. The absorbance for polymers in chlorobenzene solution was recorded with a concentration of $5.4 \cdot 10^{-3}$ mg/ml. The thin film polymer absorption was recorded on ca 28 nm thick films, whereas the blend absorption was recorded on ca. 100 nm thick films as used for solar cells and transient measurements.

Ultraviolet photon spectroscopy (UPS) measurements

Ultraviolet and X-ray photoelectron spectroscopy (UPS and XPS) experiments were performed at the endstation SurICat (beamline PM4) at the synchrotron light source BESSY II (Berlin, Germany). Spectra were collected with a hemispherical electron energy analyzer (Scienta SES 100) using excitation photon energies of 35 eV (20 eV for angular mode) (UPS) and 620 eV (XPS). The secondary electron cutoff (SECO) spectra were obtained with the sample biased at -10 V in order to clear the analyzer work function. The error of energy values reported below is estimated to be ± 0.05 eV.

FET and SCLC measurements

OFETs were prepared in bottom-gate, top-source/drain geometry. Device characteristics at room temperature were recorded using an Agilent 4155C semiconductor parameter analyzer. The measurements were performed in an inert nitrogen atmosphere. Charge carrier mobilities

were calculated from the saturation region of the output characteristics according to $I_{DS,sat} = \mu_{sat}WC_i(V_{DS} - V_0)^2/2L$, where $W=14.85$ cm and $L=100$ μm are the channel width and length, respectively, $C_i=11.9$ nF/cm² is the capacitance per unit area and V_0 is the onset voltage. The J - V characteristics to determine the space charge limited currents (SCLC) have been measured via Keithley 2400 in nitrogen atmosphere. Hole injection from PEDOT:PSS was analyzed according to Mott-Gourney law assuming Poole-Frenkel type field-dependent mobilities according to Ref 7.

Plasmon maps based on energy filtered TEM measurements

Phase separation was imaged using spectroscopic contrast in the TEM as recently demonstrated for blends of ZnPC and C₆₀.² Thin films were analyzed in a Zeiss Libra200 TEM equipped with an energy filter. By electron energy loss spectroscopy plasmon energies of 22.4 (22.2) eV and 25.1 eV were measured for pristine P-H (P-F) and PC₇₀BM, respectively. A series of energy filtered images of the blend films was recorded in the region from 19 eV to 31 eV using a 1.7 eV window and an energy increment of 0.8 eV. Plasmon spectra were extracted pixel-by-pixel from the spatially corrected image stack and adjusted for energetic drift and non-isochromaticity. Peak centers were determined by an automatic Gaussian fitting routine and laterally mapped. The range of energy scaling was set ± 0.8 eV from the center energy determined as the average energy of the plasmon maps for the individual blends with P-H and P-F processed without DIO. The average domain size was determined with open source software gwyddion. A threshold was set to the center of the energy scale shown in Figure 3. Then all data points with energy below (or above) this threshold were identified to be polymer (or PCBM) rich phases. The analysis of the mean domain size included the overall domain size divided by their number.

External quantum efficiency (EQE) measurements

The EQE was measured with monochromated light from tungsten lamp mechanically chopped to 140Hz for the detection with a lock-in amplifier. The intensity of the lamp was checked with an UV enhanced crystalline solar cell calibrated at Newport before each measurement. The quality of the EQE setup was cross checked with a KG3 filtered crystalline silicon reference solar cell calibrated at Fraunhofer ISE.

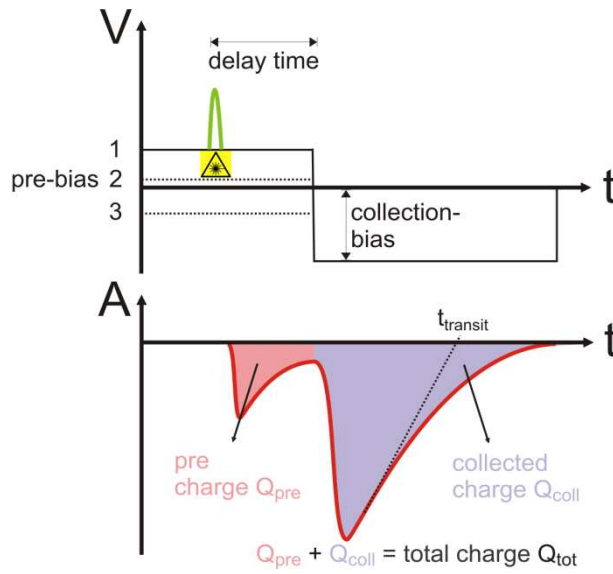
Solar cell characteristics

The solar cell characteristics were measured with an Oriel class A simulator calibrated to 100 mW/cm², the samples were temperature controlled to 20°C during measurement. The calibration of the sun simulator was done with a KG3 filtered silicon reference cell calibrated at Fraunhofer ISE. All shown data are corrected for spectral mismatch³ with a mismatch factor ranging from 0.960 to 0.963. Integrated EQE spectra were in excellent agreement with the J_{sc} measured with the solar simulator comparing identical pixel sizes.

Time delayed collection field (TDCF)

The measurement-routine is outlined in Scheme S2 and was described in detail elsewhere.⁴ The pulsed excitation (5,5 ns pulse width, 500 Hz repetition rate, 10 ns jitter) was done with a diode-pumped, Q-switched Nd:YAG laser (NT242,EKSPLA). The current through the device was measured via a 50 Ω resistor in series with the sample and was recorded with a Yokogawa DL9140 oscilloscope. The time delay between the laser pulse and the start of the collection voltage ramp was decreased to 10 ns by the following measures. First, Agilent 81150A pulse generator with a very fast slew rate of 2.5 ns was used to apply the pre- and collection bias to the sample. Second, to reduce the effect of the laser jitter on the

measurement, the pulse generator was triggered via a fast photodiode (EOT ET 2030TTL). Third, to compensate the internal latency of the pulse generator, the laser pulses were delayed with a 85 m long multimode fiber (LEONI) with respect to the first trigger diode. The pulses broadened to 6.4 ns after the fiber. A second fast photodiode (EOT ET 2030TTL) was placed after the fiber to trigger the oscilloscope. The pulse fluence was measured with a Ophir Vega power meter equipped with a photodiode sensor.



Scheme S2: Measurement-scheme for time delayed collection field (TDCF). The upper panel shows the applied voltage burst with the pre and collection bias. At pre-bias conditions, the laser pulse hits the sample and generates free charge carriers. After the delay time the collection voltage is applied to collect all photogenerated charges. The lower panel shows the corresponding current transient with the characteristic shape for ca. 150 ns delay time with two distinct current maxima. The integral over the current within the delay time is the pre-charge Q_{pre} , whereas the integral over the collection current gives the collected charge Q_{coll} . The total charge Q_{tot} is the integral over the whole current transient $Q_{tot} = Q_{pre} + Q_{coll}$.

The bimolecular recombination coefficient was iteratively calculated from the TDCF-data with equation S1.

$$Q_{coll}(t_d + \Delta t) - Q_{coll}(t_d) = -[Q_{pre}(t_d + \Delta t) - Q_{pre}(t_d)] - \gamma \frac{1}{eAd} [Q_{coll}^2(t_d) + 2Q_{coll}(t_d) \cdot Q_{dark}] \Delta t \quad (S1)$$

Here, Q_{pre} and Q_{coll} are the integrals of the photocurrent during delay and collection, respectively, d the device thickness and A the active area.⁵ Note that (S1) also considers the

density of dark charge carriers Q_{dark} due to injected charges at forward bias. An analysis of the data without considering Q_{dark} will slightly overestimate γ . The dark charge density has been measured with dark CELIV experiments for each individual pre-bias (see below). Figure S2 shows $Q_{\text{pre}}(t_d)$, $Q_{\text{coll}}(t_d)$ and $Q_{\text{tot}}(t_d)$ with the corresponding bmr-fit according to equation (S1) for different pre bias settings.

Photo-charge extraction by linearly increasing voltage (photo-CELIV)

Measurements employing the current extraction under linearly increasing voltages (CELIV) technique were realized with the same laser and excitation wavelength as used for TDCF. The linear increasing voltage ramp was applied with an Agilent 33220A wave form generator and a fast custom-built amplifier. The resulting current transients were measured with a fast current amplifier (Femto DHPA-100) and a digital oscilloscope (Yokogawa DL9040). To vary the field $F(t = t_{\text{max}})$ with t_{max} being the time with maximum photocurrent, the voltage slope A' was increased by only varying the pulse length. Note that although t_{max} decreased with increasing A' , the mobility calculated according to⁶

$$\mu = \frac{2d^2}{3A't_{\text{max}}^2[1+(0.18\frac{\Delta j}{j(0)})]} \quad (\text{S2})$$

decreased with higher $F(t = t_{\text{max}})$. The dark density Q_{dark} needed for correct calculation of the bmr-coefficient from TDCF transients has been determined via dark-CELIV. Devices were held at a pre-bias to realize steady state conditions and then the voltage ramp was applied. The dark density was determined by subtracting the capacitive current from the CELIV transient. Values for the dark charges were about $0.3 - 4 \cdot 10^{15} \text{ cm}^{-3}$. Increasing the dark charge in equation S1 artificially to values much larger than those measured by dark-CELIV led to very poor fits of the collected charge versus delay time. We, therefore, rule out that the

increase of the bmr-coefficient when the bias approaches V_{oc} as described in the main part of the paper is caused by an exceptional large dark charge.

Supplementary Figures

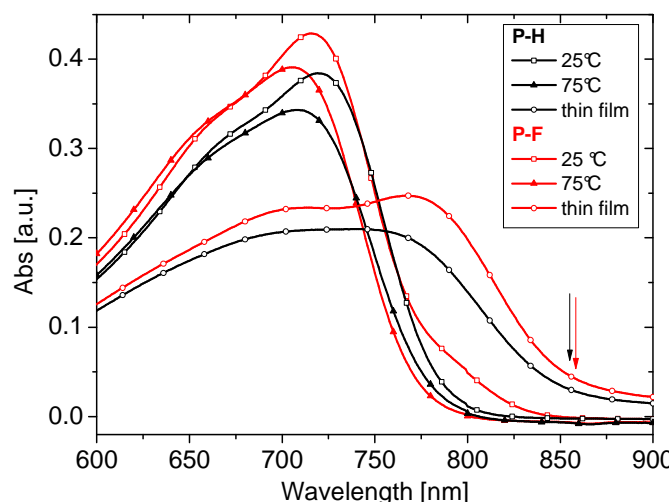


Fig. S5 Absorption spectra of $5.4 \cdot 10^{-3}$ mg/ml solutions of P-H (black) and P-F (red) in chlorobenzene measured at 25°C (solid line) and 75°C (dashed line). Also shown are film absorption spectra for identical layer thickness of 30 nm (line+ open circles). The arrows indicate the absorption onset in the film used to determine the optical band-gap as shown in Table 1 in the main text.

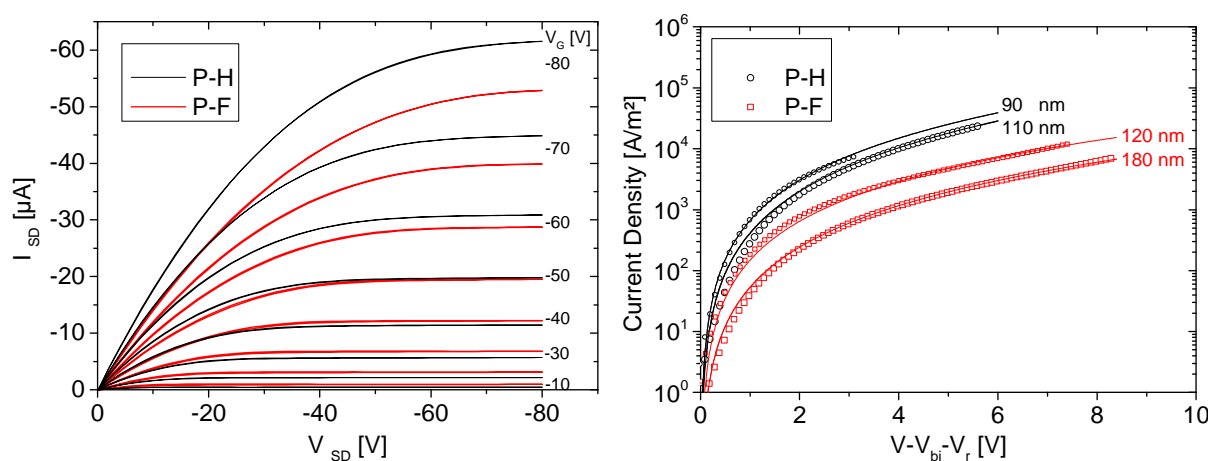


Fig. S6 (a) FET output characteristics for the polymer **P-H** (black) and **P-F** (red). Values for the hole mobility can be calculated from the saturation regime to be $1.4 \cdot 10^{-3}$ and $1.0 \cdot 10^{-3}$ cm^2/Vs for **P-H** and **P-F**, respectively. (b) J - V characteristics for the polymer **P-H** (black circles) and **P-F** (red squares) with different layer thickness as indicated. The zero field mobility was determined from SCLC measurements in the thickness range between 90 and 180 nm (not all data shown) from fits according to Poole-Frenkel type field-dependent mobility⁷ (solid lines) to be $1.0 \cdot 10^{-4}$ and $0.6 \cdot 10^{-4}$ cm^2/Vs for **P-H** and **P-F**, respectively.

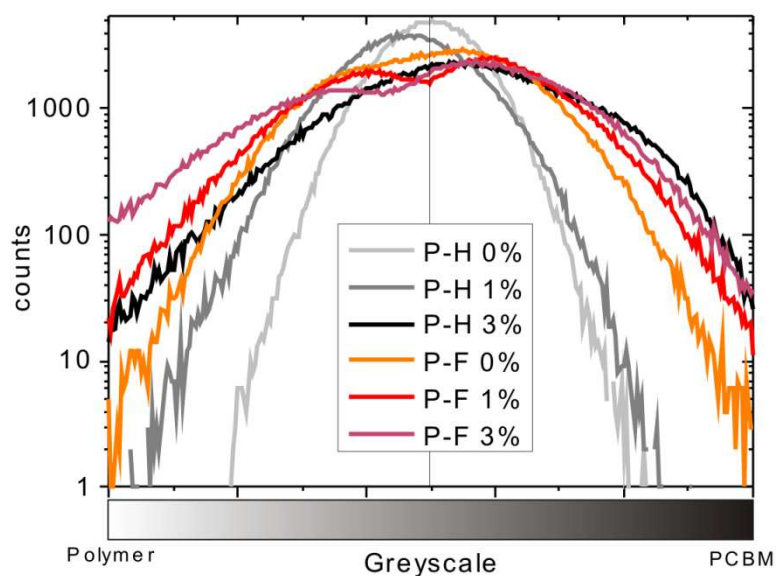


Fig. S7 Histograms (semilog plot) of the plasmon maps from Figure 3 in the main part of the paper. The x-axis shows the greyscale identical to Figure 3. Counts with darker color are assigned to PC₇₀BM and values with brighter colors are assigned to polymer rich phases. This comparison shows that with increasing amount of DIO the number of pure phases is increased as the counts for pure phases becomes higher. Also, with fluorination the polymer rich phases become more pure compared to the non fluorinated blends at identical DIO concentration.

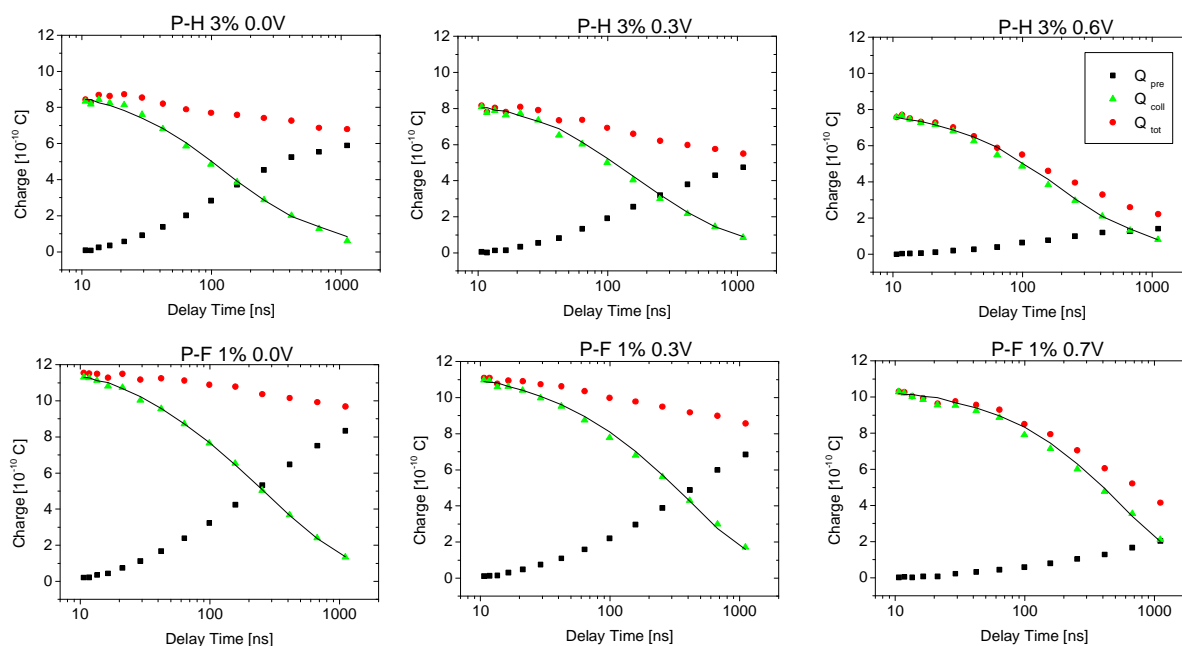


Fig. S8 Total-, pre- and collected charges extracted from transients for blends with polymer P-H and 3% DIO (upper row) and with P-F and 1% DIO (lower row) parameterized in delay time and pre-bias of 0.0 V (left column); 0.3V (middle column) and close to V_{oc} (right column). The pulse fluence was adjusted to $0.55 \mu\text{J}/\text{cm}^2$. This fluence is almost in the linear fluence versus charge density regime (see Ref 5) showing a higher signal to noise ratio for high accuracy fit-results.

Supplementary References

- (1) Cho, S.; Lee, J. K.; Moon, J. S.; Yuen, J.; Lee, K.; Heeger, A. J. *Organic Electronics* **2008**, *9*, 1107-1111.
- (2) Schindler, W.; Wollgarten, M.; Fostiropoulos, K. *Organic Electronics* **2012**, *13*, 1100-1104.
- (3) Shrotriya, V.; Li, G.; Yao, Y.; Moriarty, T.; Emery, K.; Yang, Y. *Advanced Functional Materials* **2006**, *16*, 2016-2023.
- (4) Kniepert, J.; Schubert, M.; Blakesley, J. C.; Neher, D. *The Journal of Physical Chemistry Letters* **2011**, *2*, 700-705.
- (5) Albrecht, S.; Schindler, W.; Kurpiers, J.; Kniepert, J.; Blakesley, J. C.; Dumsch, I.; Allard, S.; Fostiropoulos, K.; Scherf, U.; Neher, D. *The Journal of Physical Chemistry Letters* **2012**, 640-645.
- (6) Bange, S.; Schubert, M.; Neher, D. *Physical Review B* **2010**, *81*, 035209.
- (7) Lenes, M.; Morana, M.; Brabec, C. J.; Blom, P. W. M. *Advanced Functional Materials* **2009**, *19*, 1106-1111.